

# Directly assembled quantum dots on one dimension ordered TiO<sub>2</sub> nanostructure in aqueous solution for improving photocatalytic activity\*

HUANG Jin-zhao (黄金昭)<sup>1\*\*</sup>, KUANG Lei (况磊)<sup>1</sup>, LIU Song (刘松)<sup>1</sup>, ZHAO Yong-dan (赵永丹)<sup>1</sup>, JIANG Tao (蒋涛)<sup>1</sup>, LIU Shi-you (刘世友)<sup>1</sup>, and WEI Ming-zhi (魏明志)<sup>2</sup>

1. School of Physics and Technology, University of Jinan, Jinan 250022, China

2. School of Material Science and Engineering, Qilu University of Technology, Jinan 250353, China

(Received 5 February 2013)

©Tianjin University of Technology and Springer-Verlag Berlin Heidelberg 2013

One dimension (1D) ordered titanium dioxide (TiO<sub>2</sub>) nanostructured photocatalysts sensitized by quantum dots (QDs) are fabricated. Their morphologies, crystal structures and photocatalytic properties are characterized by scanning electron microscopy (SEM), transmission electron microscopy (TEM), X-ray diffraction (XRD) and ultraviolet-visible-near infrared (UV-vis-NIR) absorption spectroscopy, respectively. Compared with the original TiO<sub>2</sub> nanostructure, the nanostructured TiO<sub>2</sub> sensitized by QDs exhibits a good photocatalytic activity for the degradation of methyl orange (MO). The QDs with core-shell structure can reduce the photocatalytic ability due to the higher potential barrier of carrier transport in ZnS shell layer. The results indicate that the proposed photocatalyst shows promising potential for the application in organic dye degradation.

**Document code:** A **Article ID:** 1673-1905(2013)04-0241-5

**DOI** 10.1007/s11801-013-3025-3

Titanium dioxide (TiO<sub>2</sub>) is one kind of promising semiconductor material in photocatalytic degradation<sup>[1-6]</sup> because of its high photocatalytic activity, nontoxicity, strong oxidizing power, long-term chemical stability as well as low cost. Among all the nanostructured TiO<sub>2</sub> materials, vertically oriented TiO<sub>2</sub> nanostructures grown through anodization of titanium have attracted great attention<sup>[7-9]</sup> due to their high surface area and fluent charge transport. However, the wide band gap of TiO<sub>2</sub> limits its photocatalytic application, because it can only absorb about 3% of the solar ultraviolet (UV) spectrum light ( $\lambda < 400$  nm). Some efforts have been paid to enhance the visible light absorbing ability of TiO<sub>2</sub><sup>[10-16]</sup>. Among the methods, the quantum dot (QD) sensitization has shown promising characteristics.

There are some reports on the TiO<sub>2</sub> photocatalyst sensitized by QDs, but little attention has been paid on the one dimension (1D) ordered TiO<sub>2</sub> nanostructure grown directly on indium tin oxide (ITO) substrates using hydrothermal method. Besides, the investigation on the effect of core-shell QDs on the photocatalytic properties is also rare.

In this paper, QDs-assembled 1D ordered TiO<sub>2</sub> nanostructured photocatalyst is presented, and the effects of different photocatalyst structures on the photocatalytic properties for methyl orange (MO) degradation are in-

vestigated.

A TiO<sub>2</sub> sol was prepared as follows. 10 mL (29 mmol) tetrabutyl titanate (Ti(OBu)<sub>4</sub>) was dissolved in 30 mL ethanol with stirring under 25 °C, and then the glacial acetic acid was added in the solution. After stirring for 15 min, the transparent uniform faint yellow solution was obtained. Under the strong stirring, nitric acid-ethanol solution with 0.5 mL nitric acid, 10 mL ethanol and 1 mL distilled water (1–2) D·s<sup>-1</sup> was added in the above solution. After 1 h stirring, the TiO<sub>2</sub> sol was obtained. The TiO<sub>2</sub> seed layer was deposited on the ITO substrate by spin-coating method, and the optimum coating condition of a 2 cm×2 cm substrate was 3000 r/min for 30 s with acceleration time of 1 s using the TiO<sub>2</sub> sol. The seed layer was calcinated at 450 °C for 1 h in N<sub>2</sub>. ITO glass substrates (50 Ω/□) used for growing TiO<sub>2</sub> nanorod were cleaned in an ultrasonic bath with acetone, isopropanol and deionized (DI) water.

The synthesis of TiO<sub>2</sub> nanorods is as follows. 30 mL DI water was mixed with 30 mL hydrochloric acid (38% by weight). The mixture was stirred for 5 min in a teflon-lined stainless steel autoclave before the addition of 1 mL titanium butoxide. After stirring for another 5 min, the ITO substrates were placed against the wall of the teflon-liner with the conducting side facing down. The hydrothermal synthesis was conducted at 150 °C for

\* This work has been supported by the National Natural Science Foundation of China (No. 61106059), the Encouragement Foundation for Excellent Middle-aged and Young Scientist of Shandong Province (Nos.BS2011NJ003 and BS2012CL005), and the Science-Technology Program of Higher Education Institutions of Shandong Province (No.J11LA10).

\*\* E-mail: ss\_huangjinzhao@ujn.edu.cn

6 h in an electric oven. After synthesis, the autoclave was cooled to room temperature under flowing water. The ITO substrate was taken out, rinsed extensively with DI water, and calcinated at 450 °C for 1 h in N<sub>2</sub><sup>[17]</sup>.

Before synthesizing the TiO<sub>2</sub> nanotube, the ZnO nanorod was prepared firstly, and the method is introduced systematically in Ref.[18]. The synthesized ZnO nanorod arrays on ITO were immersed in the aqueous solution consisting of 0.075 mol (NH<sub>4</sub>)<sub>2</sub>TiF<sub>6</sub> and 0.2 mol H<sub>3</sub>BO<sub>3</sub> at room temperature for 0.5 h. In this solution, (NH<sub>4</sub>)<sub>2</sub>TiF<sub>6</sub> was hydrolyzed to TiO<sub>2</sub> on the surface of individual ZnO nanorods, while ZnO was dissolved simultaneously in the solution with acids produced by (NH<sub>4</sub>)<sub>2</sub>TiF<sub>6</sub> hydrolysis. The obtained TiO<sub>2</sub> nanotubes, which were top-end closed, were dipped in the glycerol solution containing 3% HF (mass percent) and 12% water for 2 min to etch away the top of the array, and then immersed in the 0.5 M H<sub>3</sub>BO<sub>3</sub> solution for 2 h to remove the residual ZnO inside the tubes. The arrays were rinsed with DI water and calcined in N<sub>2</sub> at 450 °C for 30 min<sup>[19]</sup>.

Oleic acid (OA)-capped QDs were synthesized by hot-injection method. In a three-neck flask, the 70 mL octadecene (ODE) solution containing 5.54 g OA and 0.51 g CdO was first heated to 180 °C to form a clear solution under N<sub>2</sub> atmosphere. After that, it was heated up to 270 °C. Trioctylphosphine (TOP)-Se solution, which was obtained by dissolving 1.3 mmol Se powder and 0.5 g TOP into 10 mL ODE and stirring more than 1 h, was quickly injected into the flask. Finally, methanol and acetone were added to precipitate QDs, which were then dissolved in toluene for storage<sup>[20]</sup>.

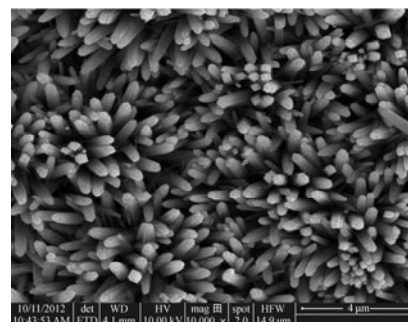
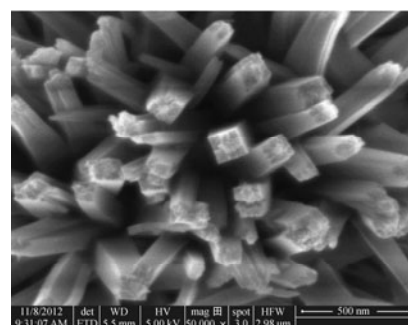
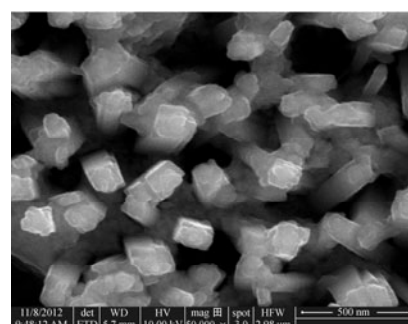
0.2 mmol CdO, 4 mmol zinc acetate and 4 mmol OA were loaded in three-neck flask, and evacuated at 150 °C for 30 min to form Zn(OA)<sub>2</sub>. Then the reactor was filled with N<sub>2</sub>, added with 15 mL ODE, and heated up to 305 °C. At this temperature, 2 mL TOP dissolving 0.1 mmol Se and 3.5 mmol S was quickly injected into the reactor. The reaction temperature was maintained at 300 °C for further growth of core-shell CdSe/ZnS QDs. After 10 min reaction, the reactor was cooled down to room temperature<sup>[21]</sup>.

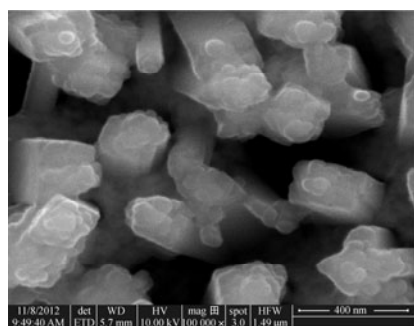
The oleic acid (OA)-capped CdSe QDs were in a toluene/acetonitrile solution with volume ratio of 1:1. The CdSe toluene/acetonitrile solution (0.2 mM) was transferred to a small vial in which two TiO<sub>2</sub> electrodes were kept at a distance of 5 mm, and a direct current (DC) voltage of 30 V was applied. After 5 min, CdSe QDs were loaded on the TiO<sub>2</sub> electrode. The adsorption of CdSe/ZnS QDs on the TiO<sub>2</sub> was made by the same way.

The structures of the samples were investigated by an X-ray diffractometer (XRD, D8 ADVANCE) using Cu K $\alpha$  radiation ( $\lambda=0.15406$  nm). The surface morphologies and microstructures were analyzed by a field-emission scanning electron microscope (FE-SEM, QUANTA 250 FEG) and transmission electron microscopy (TEM, JEM-3000F). The absorption spectrum was measured on an ultraviolet-visible-near infrared (UV-vis-NIR) spectrophotometer (TU-1901).

The photocatalytic properties were evaluated using methyl orange (MO) as a degradation dye under 300 W Hg lamp irradiation at room temperature with cooling water. MO with concentration of 15 mg/L was magnetically stirred in the dark for 12 h to reach the adsorption-desorption equilibrium, and then exposed to light. After 20 min, 5 mL solution was collected and immediately analyzed by the UV-vis-NIR spectrophotometer.

Fig.1 (a) and (b) show the SEM images of the TiO<sub>2</sub> nanorods before adsorbing CdSe QDs with different magnification times. It can be seen that the TiO<sub>2</sub> nanorods can provide larger surface area, which increases the adsorption amount of QDs and facilitates the electron transportation in the applications of photocatalytic degradation. Fig.1 (c) and (d) show the SEM images of the TiO<sub>2</sub> nanorods after adsorbing CdSe QDs with different magnification times. After sensitization of QDs, the surface of TiO<sub>2</sub> nanorods becomes rougher, and the surface of each TiO<sub>2</sub> nanorod is fully covered by QDs which can increase the photocatalytic properties.

(a) 10000 $\times$  magnification(b) 50000 $\times$  magnification(c) 50000 $\times$  magnification



(d) 100000× magnification

**Fig.1 SEM images of TiO<sub>2</sub> nanorods: (a), (b) Before and (c), (d) after sensitizing by CdSe QDs with different magnification times**

Fig.2 shows the TEM image of CdSe QDs with diameter about 4 nm uniformly dispersed in the ethanol solution, which is consistent with the result of the absorption spectrum in Fig.4(a).

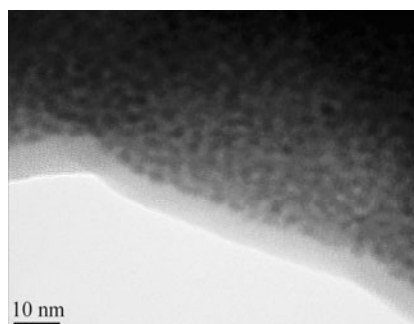
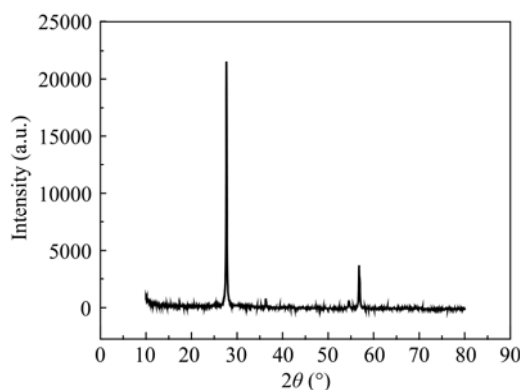


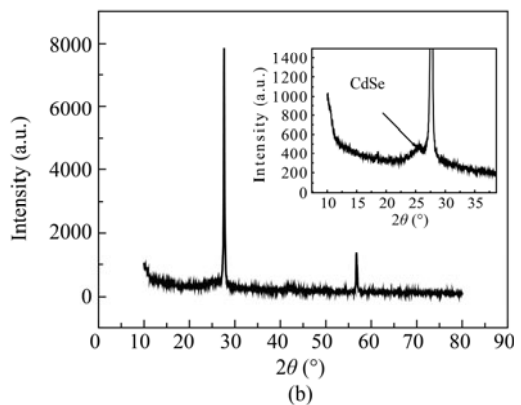
**Fig.2 TEM image of CdSe QDs with diameter about 4 nm**

The XRD is used to characterize the crystal structures of original TiO<sub>2</sub> nanorods and CdSe-QDs-sensitized TiO<sub>2</sub> nanorods. The XRD patterns of the two kinds of samples are shown in Fig.3. In Fig.3(a), all of peaks can well match with the rutile structure of TiO<sub>2</sub>, and the sharp diffraction peaks in the XRD spectrum confirm that the sample is highly crystalline. Because the TiO<sub>2</sub> peaks are high, no distinct peaks corresponding to CdSe are observed. However, some weak peaks corresponding to CdSe can be found as shown in the inset of Fig.3(b), and the diffraction pattern clearly reveals that the CdSe QDs with the wurtzite hexagonal structure are successfully assembled on the TiO<sub>2</sub> nanorods.

The wide absorption of visible light in solar spectrum is important for efficient photocatalysts. Fig.4 shows the absorption spectra of CdSe QDs and core-shell CdSe/ZnS QDs, respectively. We can see that the two kinds of QDs have the same absorption peak at 544 nm, which can facilitate the absorption of solar light. Besides, the same absorption peak is convenient for the comparison of the photocatalytic properties of the CdSe QDs and core-shell CdSe/ZnS QDs.

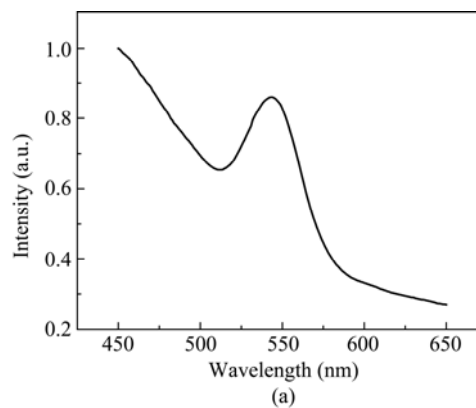


(a)

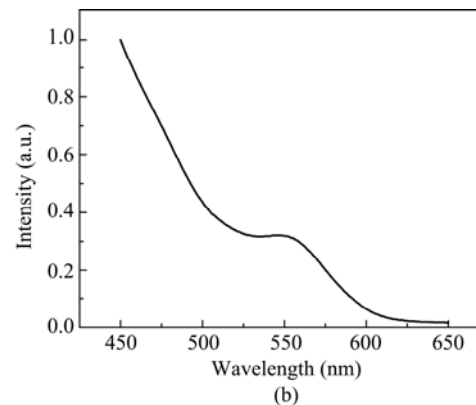


(b)

**Fig.3 XRD spectra of TiO<sub>2</sub> nanorods: (a) Before and (b) after sensitizing with CdSe QDs**



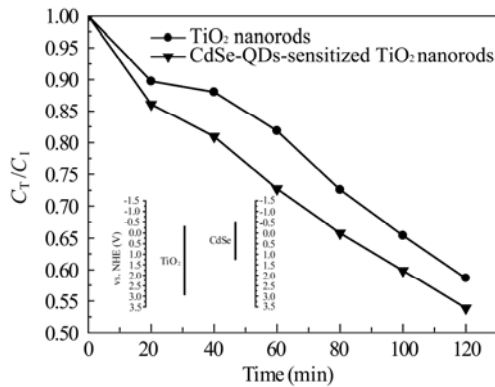
(a)



(b)

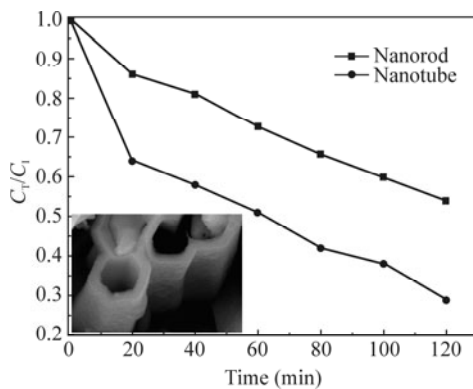
**Fig.4 UV-vis absorption spectra of (a) CdSe QDs and (b) core-shell CdSe/ZnS QDs**

Fig.5 shows the photo-degradation efficiency of MO as a function of irradiation time for different samples. For comparison, original TiO<sub>2</sub> nanorods are also examined under the same conditions. The y-axis is defined as  $C_T/C_1$ , where  $C_T$  is the absorption intensity of MO measured after different irradiated time and  $C_1$  is the initial absorption intensity. Compared with the original TiO<sub>2</sub> nanorods, the CdSe-QDs-sensitized TiO<sub>2</sub> nanorods have the stronger light-harvesting capability. This is due to CdSe has a relatively small band gap, which can make use of visible light in solar spectrum. Besides, the band alignment can enhance the carrier separation between the photo-generated electrons and holes as shown in the inset of Fig.5. Moreover, the 1D ordered TiO<sub>2</sub> nanorods can provide unblocked passageway for carrier transportation, which can reduce the recombination of carriers. So the photocatalytic activity is enhanced in degradation of MO.



**Fig.5 Photocatalytic activities of TiO<sub>2</sub> nanorods and CdSe-QDs-sensitized TiO<sub>2</sub> nanorods**

The surface area is a key factor in determining the photocatalytic properties of nanostructure material, so the QDs-sensitized TiO<sub>2</sub> nanotube photocatalyst is prepared. Fig.6 shows the photocatalytic activities of CdSe-sensitized TiO<sub>2</sub> nanorods and nanotube. It can be seen that the nanotube can enhance the photocatalytic activity to some extent, which results from the increased active surface area of photocatalyst.



**Fig.6 Photocatalytic activities of CdSe-sensitized TiO<sub>2</sub> nanorods and CdSe-sensitized TiO<sub>2</sub> nanotube (The inset is the SEM image of TiO<sub>2</sub> nanotube.)**

Fig.7 shows the photo-degradation activity of CdSe/ZnS-QDs-sensitized TiO<sub>2</sub> nanorods. Compared with the CdSe-QDs-sensitized TiO<sub>2</sub> nanorods, the core-shell-QDs-sensitized nanorods present lower photocatalytic performance, under the condition that both of the two kinds of QDs have the same absorption peak (as shown in Fig.4). This is maybe due to the higher carrier transport potential barrier of ZnS shell layer. The inset of Fig.7 shows the band diagrams of TiO<sub>2</sub>, CdSe and ZnS. The band gap of CdSe is smaller than that of ZnS, so the separation of carriers is reduced, and the photocatalytic ability is decreased<sup>[22]</sup>.

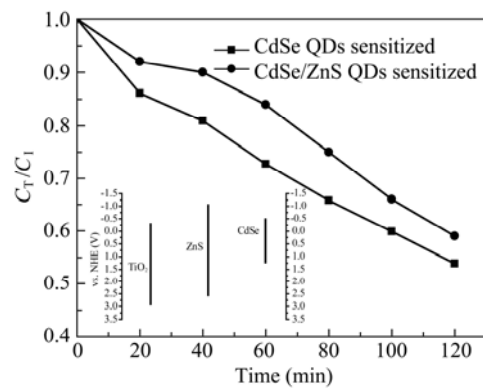


**Fig.7 Photocatalytic activities of CdSe-QDs-sensitized TiO<sub>2</sub> nanorods and CdSe/ZnS-QDs-sensitized TiO<sub>2</sub> nanorods**

In addition, the photocatalyst grown on ITO substrates makes the collection and recycle of the photocatalyst easier, because it can be directly taken out and washed by water. Moreover, the photocatalytic process neither loses the photocatalyst nor brings new pollution because of the tight connection between the photocatalyst and ITO.

The photocatalyst is prepared by assembling QDs onto 1D ordered TiO<sub>2</sub> nanostructure, and the photocatalytic properties for MO degradation are investigated by SEM, TEM, XRD and UV-vis-NIR absorption spectroscopy. The results show that QDs-sensitized TiO<sub>2</sub> nanostructure is more favourable for the photo-degradation, because of the larger optical absorption cross section, the easier electron-hole charge separation, the smaller band gap and the easier carrier transportation. Photocatalytic ability of core-shell-QDs-sensitized TiO<sub>2</sub> nanostructure is lowered, because of the higher carrier transport barrier of ZnS shell layer. Furthermore, the QDs-sensitized TiO<sub>2</sub> nanostructure directly grown on ITO substrates makes the collection and recycle of the photocatalyst easier. The results provide a useful clue on structure design and selection of the 1D ordered TiO<sub>2</sub> nanostructured sensitizers based on photocatalyst.

**References**

[1] Y. X. Tang, P. X. Wee, Y. K. Lai, X. P. Wang, D. G.

- Gong, Pushkar D. Kanhere, T. -T. Lim, Z. L. Dong and Z. Chen, *J. Phys. Chem. C* **116**, 2772 (2012).
- [2] B. S. Liu, K. Nakata, S. H. Liu, M. Sakai, T. Ochiai, T. Murakami, K. Takagi and A. Fujishima, *J. Phys. Chem. C* **116**, 7471 (2012).
- [3] P. Chowdhury, J. Moreira, H. Gomaa and K. Ray Ajay, *Ind. Eng. Chem. Res.* **51**, 4523 (2012).
- [4] F. J. Zhang, X. W. Xu, W. H. Tang, J. Zhang, Z. L. Zhuo, J. Wang, J. Wang, Z. Xu and Y. S. Wang, *Sol. Energ. Mat. Sol. C.* **95**, 1785 (2011).
- [5] Z. G. Chen, P. Y. Liu, L. T. Hou, W. J. Mai and B. Wu, *Optoelectronics Letters* **8**, 93 (2012).
- [6] P. Niu and J. C. Hao, *Langmuir* **27**, 13590 (2011).
- [7] F. X. Xiao, *J. Mater. Chem.* **22**, 7819 (2012).
- [8] X. J. Xu, C. C. Tang, H. B. Zeng, T. Y. Zhai, S. Q. Zhang, H. J. Zhao, Y. Bando and D. Golberg, *ACS Appl. Mater. Interfaces* **3**, 1352 (2011).
- [9] J. J. Liao, S. W. Lin, L. Zhang, N. Q. Pan, X. K. Cao and J. B. Li, *ACS Appl. Mater. Interfaces* **4**, 171 (2012).
- [10] W. j. Li, D. Z. Li, Z. X. Chen, H. J. Huang, M. Sun, Y. H. He and X. Z. Fu, *J. Phys. Chem. C* **112**, 14943 (2008).
- [11] D. -Lin. Shieh, Y. -S. Lin, J. -H. Yeh, S. -C. Chen, B. -C. Lin and J. -L. Lin, *Chem. Commun.* **48**, 2528 (2012).
- [12] B. Mukherjee, York R. Smith and V. Subramanian, *J. Phys. Chem. C* **116**, 15175 (2012).
- [13] F. Y. Shen, W. X. Que, Y. L. Liao and X. T. Yin, *Ind. Eng. Chem. Res.* **50**, 9131 (2011).
- [14] C. Ratanatawanate, A. Bui, K. Vu and Jr. Kenneth J. Balkus, *J. Phys. Chem. C* **115**, 6175 (2011).
- [15] S. Cho, J. -W. Jang, J. W. Kim, J. S. Lee, W. Choi and K. -H. Lee, *Langmuir* **27**, 10243 (2011).
- [16] M. R. Dalai, Z. W. Yan and L. Shi, *Optoelectronics Letters* **8**, 224 (2012).
- [17] B. Liu and Eray S. Aydil, *J. Am. Chem. Soc.* **131**, 3985 (2009).
- [18] X. W. Sun, J. Z. Huang, J. X. Wang and Z. Xu, *Nano Lett.* **8**, 1219 (2008).
- [19] C. K. Xu and D. Gao, *J. Phys. Chem. C* **116**, 7236 (2012).
- [20] J. Chen, J. L. Song, X. W. Sun, W. Q. Deng, C. Y. Jiang and W. Lei, *Appl. Phys. Lett.* **94**, 153115 (2009).
- [21] J. Kwak, W. K. Bae, D. Lee, I. Park, J. Lim, M. Park, H. Cho, H. Woo, Do Y. Yoon, K. Char, S. Lee and C. Lee, *Nano Lett.* **12**, 2362 (2012).
- [22] A. Kudo and Y. Miseki, *Chem. Soc. Rev.* **38**, 253 (2009).